Journal of Zhejiang University-SCIENCE A 2026 27(10):1095-1106
www.jzus.zju.edu.cn; www.springer.com/journal/11582
E-mail: jzus_a@zju.edu.cn

Research Article
https://doi.org/10.1631/jzus.A2500648

Check for updates

High-sensitivity flexible iontronic pressure sensor for pulse signal detection and underwater intelligent communication

Menghui XIANG[1,2*], Cong ZHAI[2*✉], Congcong HAO[3*], Guirong WU[1], Jin CHAI[2,4], Yunlong ZHAO[1], Zekai HUANG[1], Bin YAO[1,2], Heying ZHANG[3], Mengran LIU[5], Lei NIE[5], Xiewen WEN[6], Chenyang XUE[1,2], Libo GAO[1✉]

[1]*Discipline of Intelligent Instrument and Equipment, Pen-Tung Sah Institute of Micro-Nano Science and Technology, Xiamen University, Xiamen 361005, China*
[2]*Laoshan Laboratory, Qingdao 266237, China*
[3]*Key Laboratory of Instrumentation Science & Dynamic Measurement, North University of China, Taiyuan 030051, China*
[4]*College of Chemistry and Chemical Engineering, Xiamen University, Xiamen 361005, China*
[5]*Key Lab of Modern Manufacture Quantity Engineering, School of Mechanical Engineering, Hubei University of Technology, Wuhan 430068, China*
[6]*Department of Industrial and Systems Engineering, University Research Facility in 3D Printing, State Key Laboratory of Ultra-precision Machining Technology, The Hong Kong Polytechnic University, Hong Kong 999077, China*

Abstract: Flexible pressure sensors have become pivotal in the advancement of wearable electronics and underwater monitoring, particularly when augmented by artificial intelligence. Nevertheless, the development of a unified sensing platform capable of seamless operation in both health monitoring and underwater communication remains a significant challenge. To address this issue, a highly sensitive flexible iontronic pressure sensor featuring a micro-pyramidal architecture was developed. The device is fabricated using molding involving a bespoke composite ink comprising carbon nanotubes (CNTs) and ionic liquid as the sensing layer. This layer is then sandwiched between screen-printed silver electrodes. The sensor demonstrated exceptional performance metrics, including high sensitivity (370 kPa^{-1}), rapid response and recovery times (20 ms), and outstanding reliability (about 20000 cycles). In the domain of wearable health monitoring, the sensor demonstrated its capacity to discern faint human pulse signals, facilitating the acquisition of high-fidelity pulse waveforms. Concurrently, within the domain of underwater intelligent communication, the sensor was used to detect Morse code signals, which were then accurately classified by a deep learning algorithm. This work not only validates the sensor's high performance but also demonstrates its dual functionality, seamlessly connecting human healthcare with intelligent underwater interaction and significantly broadening the scope of flexible sensing applications.

Key words: Flexible pressure sensor; Underwater sensing; Iontronic sensor; Machine learning

1 Introduction

Recent years have seen a significant advancement in the field of flexible sensors, largely driven by their extensive applications in human physiological monitoring (Yang ZK et al., 2023; Teng et al., 2024; Zhao YL et al., 2024b) and motion tracking (Ren et al., 2022; Liu et al., 2024; Zhang et al., 2024; Zhu et al., 2024; Liang et al., 2025). Concurrently, continuous technological innovations have significantly enhanced their sensitivity and operational stability. In essence, flexible sensors substitute conventional rigid materials with compliant counterparts (Min et al., 2023; Lin et al., 2025), encompassing piezoresistive (Li ZW et al., 2025; Xiang QX et al., 2025), capacitive (Ma et al., 2024; Liu et al., 2026), and triboelectric principles (Chang et al., 2026; Sun et al., 2026). Capacitive sensors have attracted particular attention due to their

✉ Cong ZHAI, OliverChild@hotmail.com
Libo GAO, lbgao@xmu.edu.cn
* These authors contributed equally to this work
Menghui XIANG, https://orcid.org/0000-0002-1892-9673
Cong ZHAI, https://orcid.org/0000-0002-7288-2968
Libo GAO, https://orcid.org/0000-0002-5964-2337

Received Dec. 11, 2025; Revision accepted Feb. 4, 2026;
Crosschecked Apr. 29, 2026; Online first May 25, 2026

© Zhejiang University Press 2026

structural simplicity, low power consumption, and excellent stability. Li KX et al. (2025) proposed a flexible capacitive sensor with a micro-pyramidal structure that can detect subtle physiological signals, such as heart rate, facial expressions, and joint movements. Liu et al. (2026) attained a substantial advancement in sensitivity by devising a hybrid system incorporating carbon nanotubes (CNTs) and thermally expandable microspheres. They reported a two-fold enhancement in sensitivity compared with systems that used CNTs alone. In addition, Kurup et al. (2022) advanced material design through the use of graphene-coated polydimethylsiloxane (PDMS) porous foam, thereby fabricating a sensor capable of detecting minute pressure variations. This finding underscores the sensor's potential for wearable biomedical applications.

However, conventional parallel-plate capacitive sensors are subject to inherent limitations, including relatively low sensitivity (typically less than 1 kPa^{-1}) and instability due to environmental factors such as humidity, temperature, and parasitic capacitance. To address these challenges, iontronic sensing has emerged as a transformative paradigm (Nie et al., 2012, 2015; Cheng et al., 2022; Guo et al., 2025). This approach facilitates the formation of electrical double layers (EDLs) at the interface, generating nanoscale double-layer capacitances. This mechanism yields remarkably elevated capacitance per unit area (frequently more than 1 $\mu F/cm^2$) and sensitivity (typically between 10 and 100 kPa^{-1}), demonstrating substantial superiority over conventional parallel-plate structures. Consequently, this mechanism has prompted many researchers to focus on the higher sensitivity of ion-based sensors and conduct related application research. For instance, Yang ZK et al. (2024) focused on enhancing the sensitivity of ion-based pressure sensors. They engineered an ultra-sensitive pressure sensor using thermally expandable microspheres and constructed a flexible array capable of high-resolution radial artery pulse detection. Subsequent studies prompt a gradual shift in research focus from the initial emphasis on basic performance enhancements, such as sensitivity, to multifunctional integration and intelligent system applications. For instance, Yang QQ et al. (2023) initiated research on multifunctional integration and developed an ion-based sensor with temperature and pressure decoupling, which demonstrated significant application value in the field of human–machine interfaces (HMIs). In their subsequent research, they integrated intelligent system applications, developed a machine learning-enhanced modular ionic skin, and established a versatile framework for operator identification and robotic tactile recognition in next-generation HMI applications (Yang et al., 2025). Zhao YL et al. (2024a) also conducted research on multifunctional integration and intelligent system applications based on high sensitivity. These applications integrate multi-channel active pressure for signal acquisition and perform personalized blood pressure prediction based on artificial intelligence (AI).

Concurrently, flexible pressure sensors have been increasingly adapted for underwater applications, presenting both unique opportunities and challenges within aquatic environments. The implementation of sensors in underwater environments requires high standards of waterproofing, pressure resistance, signal fidelity, and associated properties. Notably, the ability to withstand submersion represents a pivotal challenge. At present, technical solutions that demonstrate effective waterproof capabilities mainly encompass three methods: gels, mechanical structures, and waterproof materials. For instance, Yang CX et al. (2024) fabricated hydrogel electrodes composed of MXene and ionic liquid, integrating them into a sensor capable of continuous operation for a period of 60 d. Their device offers novel pathways for flow-field monitoring and aquatic tagging. Zhao JW et al. (2024) proposed a capacitive hydrophone (CH) based on mechanical structure encapsulation, specifically designed for high-sensitivity detection of low-frequency underwater acoustic signals, demonstrating the ability of a CH to detect ships and underwater sounds. In our previous research, we fabricated two types of underwater capacitive pressure sensors based on waterproof material encapsulation. One of these sensors was designed for monitoring in shallow seas, while the other was designed for monitoring in deep seas (Wang et al., 2024; Xiang MH et al., 2025). A comparative analysis of the three underwater encapsulation methods revealed that the gel-based process is relatively cumbersome, while the mechanical structure-based approach necessitates the design of a tight waterproof structure and the processing of metal parts. The encapsulation of flexible and waterproof materials has seen a surge in popularity, owing to its numerous advantages, including ease of access and preparation. This method has been shown to achieve a balance between critical characteristics such as cost, pressure resistance, and signal fidelity. Nevertheless, research in this domain exhibits certain

deficiencies with respect to cross-media generalization and integrated land–sea intelligent sensing platforms. Most reported sensors can perform distinct functions in two distinct domains: underwater communication and physiological health monitoring. While these limitations do not significantly impact the fundamental capabilities of sensors, they do impose constraints on their versatility and range of application. The sensor described in this paper represents a development of our previous research on underwater pressure sensors. On the one hand, it can be used in both air and underwater media after undergoing waterproof encapsulation. On the other hand, the concurrent implementation of underwater communication and human physiological signal monitoring enables the sensor to assume a more pivotal role in swimming, diving, and underwater tasks, such as the timely provision of alerts to divers in cases of imminent peril.

In this study, sensor electrodes were fabricated using screen-printed conductive silver paste, while the ion-sensitive layer was mainly formulated from a composite ink comprising CNTs and ionic liquid. The sensor layered structure and simplified manufacturing method are shown in Fig. 1a. To enhance sensitivity, a micro-pyramidal architecture was engineered onto the sensing layer via a molding process, followed by laser cutting for device shaping. This fabrication strategy not only supports high customization but also facilitates scalable batch production, significantly widening the sensor's potential adoption. The device demonstrates robust functionality across diverse environments, leveraging its exceptional sensitivity. The sensor can effectively detect different signals when attached in different places (Figs. 1b and 1c). The application of principles derived from traditional Chinese medicine (TCM)—specifically the technique of using graduated pressure to ascertain the optimal detection pressure—has facilitated the acquisition of high-fidelity pulse waveforms. To extend the operational scope of the sensor to aquatic environments, the sensor was encapsulated in an ultra-thin and medical-grade adhesive film. In subsequent experiments conducted underwater (Fig. 1d), the sensor showed the capacity to sense Morse code signals, which were accurately decoded by means of a deep learning algorithm. The integration of flexible sensing with intelligent signal processing has the potential to significantly expand the application scope of the sensor.

2 Methods

2.1 Materials and equipment

The electrode material selected for the sensor was stretchable conductive silver paste (Shanghai Ouyi Organic Photoelectric Materials Co., Ltd., China). The composition of the sensor's sensitive layer material included a blend of thermoplastic polyurethane (TPU) (Dongguan Zhangmutou Ruixiang Polymer Materials Operation Department, China), CNTs (Suzhou Carbon Peak Graphene Technology Co., Ltd., China), and ionic liquid (1-ethyl-3-methylimidazolium bis(trifluoromethylsulfonyl)imide, EMIM, obtained from Shanghai Aladdin Biochemical Technology Co., Ltd., China). The organic solvent used was N,N-dimethylformamide (DMF, Shanghai Aladdin Biochemical Technology Co., Ltd., China).

A series of experiments was conducted to assess the mechanical and electrical properties of the sensor. The experimental apparatus included a digital inductance, capacitance, and resistance (LCR) meter (TH2840B, Changzhou Tonghui Electronic Co., Ltd., China) and a mechanical testing machine (ZQ-990B, Dongguan Zhiqu Precision Instrument Co., Ltd., China). The electrodes, sensitive layer structure, and element distribution were observed using a scanning electron microscopy (SEM, G300, Carl Zeiss AG, Germany).

2.2 Sensor fabrication

The simplified sensor fabrication process is illustrated in Fig. 1a (for more details, refer to Fig. S1 of the electronic supplementary materials (ESM)). First, polyethylene terephthalate (PET) substrates were laser-cut into the desired geometry and plasma-treated to enhance surface adhesion. Conductive silver paste was then deposited onto the substrates via screen printing, followed by curing in a vacuum oven at 80 ℃ for 10 min to finalize the electrodes. The preparation of the ionic sensing membrane involved the dissolution of TPU pellets in DMF at a ratio of 1:5 under magnetic stirring (80 ℃; 220 r/min) for a duration of 30 min, with the objective of achieving a homogeneous solution. Subsequently, 1.0 mL of the ionic liquid EMIM was added dropwise to prevent agglomeration. Finally, CNTs were introduced to the mixture. The slurry was stirred at a rate of 200 r/min for a period of 10 min, and then subjected to high-frequency ultrasonication to ensure a uniform dispersion of the conductive



Fig. 1 Overall application and preparation process of the sensor: (a) sensor layered structure diagram and detailed manufacturing process; (b and c) schematic diagrams of sensor attached places; (d) schematic diagram of underwater communication

fillers. The resulting ionic composite was cast into a prefabricated mold and subjected to a spin-coating process, which ensured uniform film thickness. Following a drying process in a vacuum oven at 80 °C for 30 min, the freestanding ionic film was peeled from the mold. The sensor assembly was completed by the methodical placement of the ionic film between two silver electrodes, with the use of 3M double-sided adhesive tape functioning as a spacer to delineate the active sensing area and facilitate adhesion of the layers. Fig. 1a provides an exploded view of the sensor layered architecture. To optimize pressure sensitivity, a micro-pyramidal structure was engineered within the sensing layer using a molding technique. An optical photograph of the fully fabricated sensor is presented in Fig. 2a. The microstructural details are highlighted in Fig. 2b, where a cross-sectional optical micrograph captures the well-defined pyramidal profile of the ionic membrane. SEM further elucidates this morphology in Fig. 2c, confirming the structural uniformity of the pyramids. After the morphological characterization, energy dispersive spectroscopy (EDS) was used to

evaluate the elemental composition. To eliminate potential topographic artefacts in the EDS mapping caused by the height variation of the micro-pyramids, a flat and microstructure-free film was synthesized for this analysis. The unique N and F elements present in the ionic liquid exhibit a uniform and dense distribution throughout the sensitive layer matrix (Fig. S2 of the ESM), further verifying the uniform distribution of ionic liquid and CNTs in the matrix.

2.3 Analysis of sensing mechanism

The sensing mechanism was elucidated using a dual-perspective analysis, integrating microscopic interfacial principles with macroscopic contact mechanics. Microscopically, the incorporation of ionic liquid fundamentally transforms the device from a conventional parallel-plate capacitor into an iontronic sensor. Unlike in conventional architectures, the mobile ions present within the electrolyte facilitate the formation of EDLs at the electrode interfaces, with charge separation occurring on the nanometer scale. This mechanism yields an ultra-high specific capacitance (capacitance per unit area). Consequently, the total detected capacitance is contingent on the effective interfacial contact area. The sensor achieves baseline capacitance values in the nano-Farad (nF) range because of the super-capacitive effect. This is significantly higher than the pico-Farad (pF) range typical of parallel-plate counterparts. This high intrinsic capacitance has been shown to significantly reduce the device's impedance, thereby minimizing its susceptibility to parasitic electromagnetic noise from the environment. Consequently, this results in a marked enhancement of both the signal-to-noise ratio and the resolution of the signal. Moreover, the tubular topology of the CNTs facilitates efficient loading and retention of the ionic liquid, ensuring robust ionic transport. For clarity, the schematic diagram has been simplified by depicting only CNTs, positive ions, and negative ions in the sensor sensitive layer (Fig. 2d). On a macroscopic level, the engineered pyramidal microstructure exerts a regulatory influence on the dynamic response of the contact area. The sensing principle is predicated on the modulation of the ion–electron interface under mechanical load. As the pressure increases, the contact area between the pyramidal microstructure and the bottom electrode evolves through

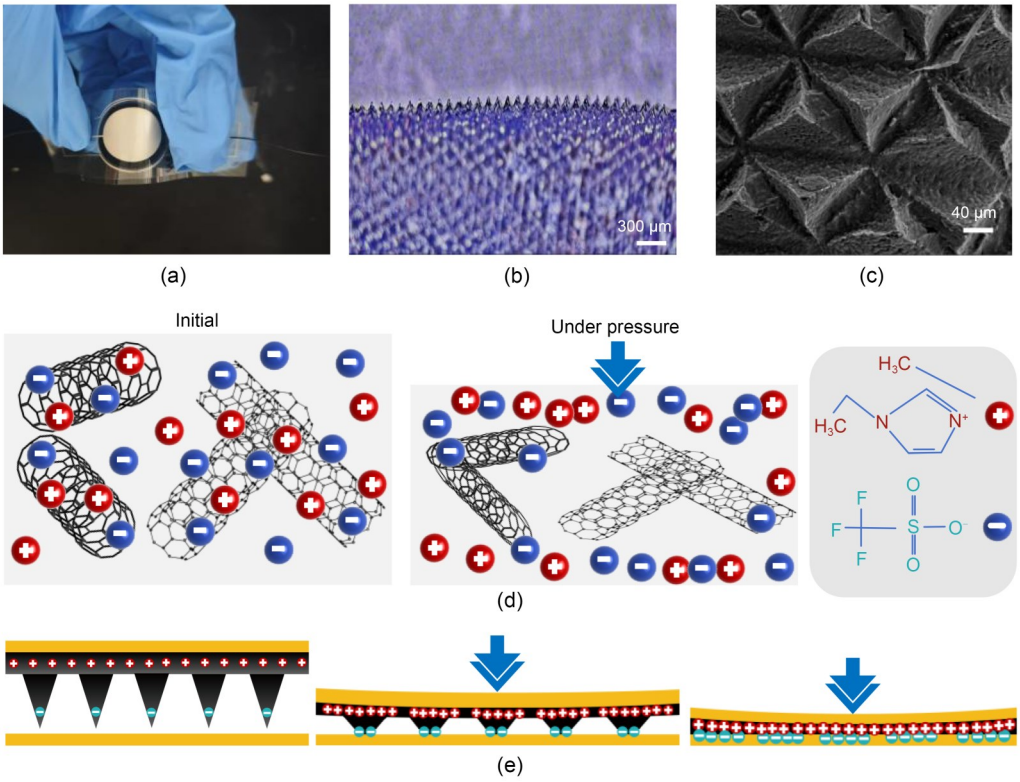


Fig. 2 (a) An optical photograph of the sensor; (b and c) microstructural details of sensitive layer; (d) schematic diagram of sensor micro-mechanism; (e) non-linear variation in contact area

distinct regimes: initial apex contact, progressive sidewall deformation, and eventual structural saturation (Fig. 2e). This characteristic deformation behavior gives rise to a non-linear variation in contact area, which initially grows gradually, followed by a rapid expansion, and finally plateaus. This variation aligns precisely with the measured sensitivity curve of the sensor. In the initial phase, the contact area between the pyramid microstructure and the electrode is comparatively small, thus resulting in minimal alterations. The mid-term stage is characterized by the most significant changes in the contact area between the pyramid microstructure and the electrode, thereby optimizing sensitivity. The subsequent phase is known as the structural saturation stage, during which the sensitivity is the least optimal.

3 Results and discussion

3.1 Sensor performance

The final sensor architecture was established through a series of comparative experiments aimed at optimizing the design. Initially, conductive silver paste was selected for the electrodes due to its excellent rheological properties for screen printing and scalability for mass production. To enhance performance, a hybrid composite ink of ionic liquid and CNTs was used. This formulation transformed the device from a conventional parallel-plate capacitor into an iontronic sensor, thereby significantly enhancing sensitivity and immunity to environmental interference. To identify the optimum compromise between cost and performance, composites with various concentrations of CNTs were evaluated. The sensor attained optimal functionality with a CNT loading of 0.10 g (3.8%, mass fraction) (Fig. 3a). This effect can be attributed to two main factors. Firstly, an increase in the content of CNTs will lead to a continuous increase in the conductivity of the ion-sensitive layer, which may result in a larger initial capacitance of the sensor. Consequently, a higher requirement is placed on the large capacitance change required for the sensor's high sensitivity. Conversely, an increased quantity of CNTs may result in their disparate dispersion within the ion slurry, which may, in turn, diminish the deformability and mechanical stability of the ion-sensitive layer. Following confirmation of the optimal content of CNTs, an investigation was conducted into the content of the ionic liquid in the sensitive layer. With a constant CNT content, sensitive layer slurries were prepared using 0.5, 1.0, or 2.0 mL of ionic liquid. A comprehensive array of experimental findings is given in Fig. S3 of the ESM. The results showed that 1.0 mL of ionic liquid was the optimal volume within the experimental parameters delineated in this study. Two potential explanations for this phenomenon are posited. First, an increase in the amount of ionic liquid may increase the initial capacitance of the sensor. This, in turn, necessitates a greater change in capacitance to achieve high sensitivity. Second, an increase in the amount of ionic liquid may result in a decrease of the elastic modulus of the composite material. This decrease has the potential to narrow the high sensitivity range of the material and facilitate the attainment of saturation. The sensitivity profile of the sensor exhibits three distinct regimes, up to 370 kPa^{-1} (Fig. 3b) (for more details of the sensitivity mechanism, please refer to Section 2.3). In addition, the transient characteristics of the sensor were evaluated, which are critical components for effective real-time monitoring. The device exhibits rapid response and recovery times, with both measuring about 20 ms (Fig. 3c). The limit of detection (LOD) was determined through the application of subtle pressure using lightweight aluminum weights. The sensor demonstrated its capability to capture weak physiological signals, resolving a pressure as low as 40 Pa (Fig. 3d). Furthermore, an assessment was conducted on the sensor's dynamic range and stability. Step-loading tests (Fig. 3e and Fig. S4 of the ESM) confirmed the robustness of the signal stability across various pressure gradients. A comparison with other published sensors (Fig. 3f) showed that our sensor achieves a superior balance between high sensitivity and a broad detection range. Finally, the long-term durability of the sensor was validated through the implementation of cyclic loading tests (Fig. 3g); the sensor showed stable performance with negligible signal drift after about 20000 cycles at 60 kPa, thereby indicating excellent operational reliability. The capacitive response of the sensor degraded after a certain number of cycles. The main cause of this degradation presumably is fatigue in the sensitive layer. Due to the relatively high velocity and substantial pressure applied during testing, the sensor was subjected to extreme and harsh conditions that it would rarely encounter in normal use. This resulted in irreversible deformation or cracks in the microstructure of the sensitive layer

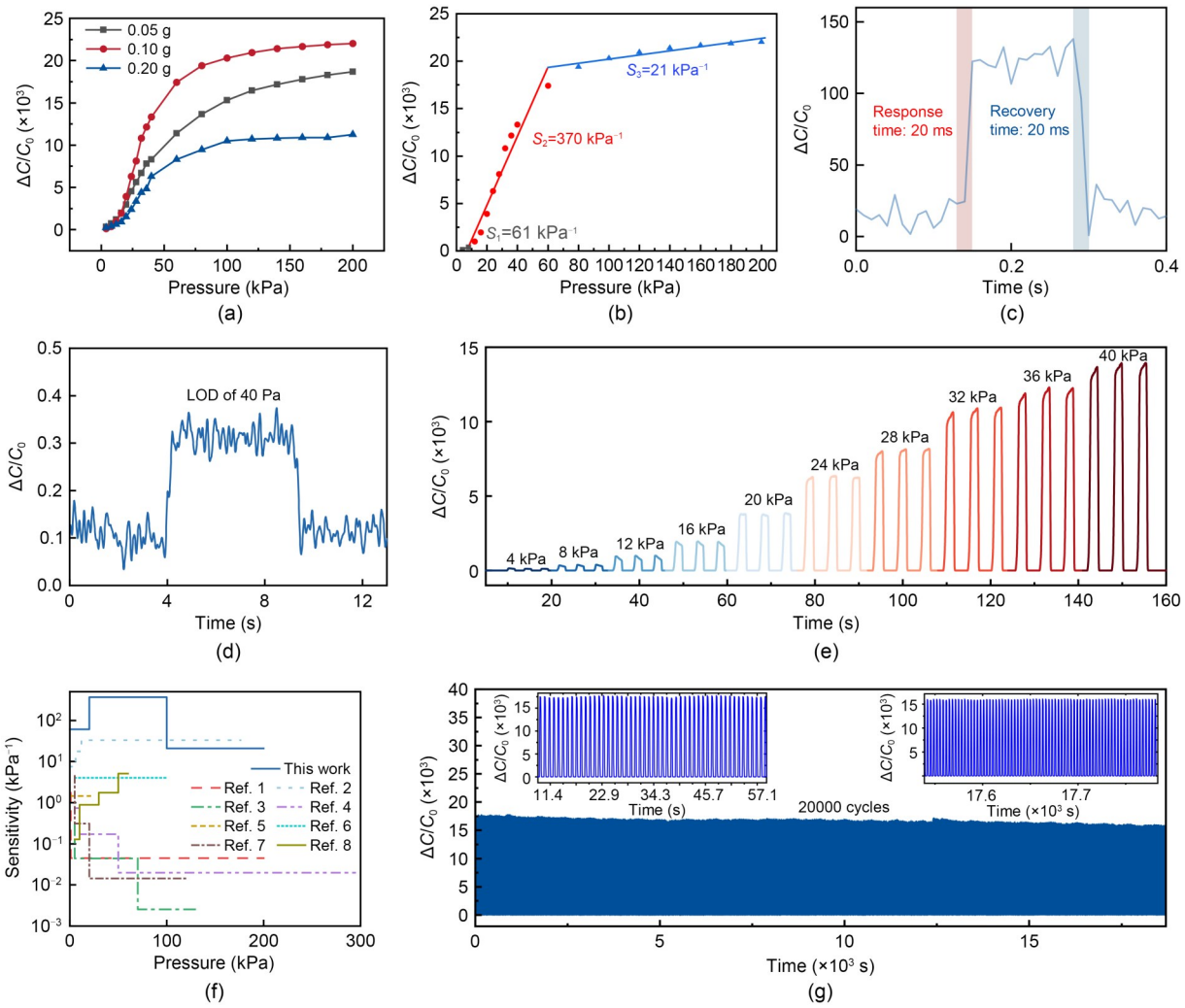


Fig. 3 (a) Sensor performance at different concentrations of CNTs; (b) sensor sensitivity profile exhibiting three distinct regimes; (c) response and recovery times of the sensor; (d) LOD of the sensor; (e) assessment on the sensor's dynamic range and stability; (f) performance comparison with other published sensors; (g) long-term durability of the sensor by cyclic loading tests. ΔC and C_0 are the change in capacitance and initial capacitance, respectively; S_1, S_2, and S_3 are the sensitivities of sensors at initial apex contact, progressive sidewall deformation, and eventual structural saturation, respectively. Refs. 1–8 correspond to Yang et al. (2019), Lu et al. (2021), Hong et al. (2023), Lv et al. (2023), Cetin et al. (2024), Guo et al. (2024), Jin et al. (2024), and Wang et al. (2025), respectively

under cyclic pressure, leading to reduced compressibility and resilience, and further performance degradation. Note that even in the presence of degradation, the performance showed a notable degree of sensitivity, and so such degradation should not have a substantial impact in practical application scenarios.

3.2 Pulse signal detection

The pulse signal originating from the heart is a significant physiological signal used for measuring human health. The signal is not only directly related to heart rate but also has the capacity to provide a more comprehensive reflection on the health status of the human heart. In TCM, pulse diagnosis has a particularly significant emphasis. To rigorously validate the sensor's pulse detection capabilities, both simulated equipment tests and in vivo human trials were conducted. Initially, a commercial pulse signal generator (Fig. 4a) was used to assess the response to standardized waveforms. Despite the simulator producing signal amplitudes that are considerably higher than those of typical human pulses, the sensor accurately resolved the waveform features. The characteristics of the pulse signal were clearly visible (Fig. 4b).

Subsequently, an evaluation was conducted of the sensor's capacity to capture subtle arterial pulses from a human subject. This application was inspired by the variable-pressure techniques used in TCM pulse diagnosis. Accordingly, graduated static pressure was applied to the radial artery. The sensor produced waveforms of high fidelity across a range of pressure levels (Figs. 4c–4e). Quantitative analysis revealed that the pulse signal amplitude showed a non-monotonic trend, initially increasing and then decreasing as pressure rose. This observation is consistent with the TCM principle of an optimal pulse pressure for maximizing diagnostic accuracy. Performance tests were also conducted on the sensor under bending conditions (Fig. S5 of the ESM). The sensor showed a higher output under bending conditions when subjected to the same pressure. This phenomenon can be attributed, at least in part, to the sensor's increased deformation when subjected to bending conditions, which in turn leads to a more substantial capacitance change. Nevertheless, this does not have a substantial impact on the practical application scenarios of the sensor. The analysis of the experimental results indicates that sensor has the capacity to obtain human pulse signals in a variety of states, which can make a significant contribution to long-term physiological signal monitoring in future health scenarios.

3.3 Underwater intelligent communication

Following the detection of human physiological signals, the sensors were encapsulated for the purpose of testing their application in underwater intelligent communication. The underlying objective of this study was to explore the potential of underwater encapsulation to broaden the operational scope of the sensors, thereby facilitating their effective use in both air and underwater environments. The construction of the underwater intelligent communication system was intended to provide further verification of the robustness of the sensors in complex underwater environments and their ability to integrate with machine learning systems. The medical waterproof tape used in this study boasts several noteworthy characteristics, including its ultra-thin profile, remarkably strong

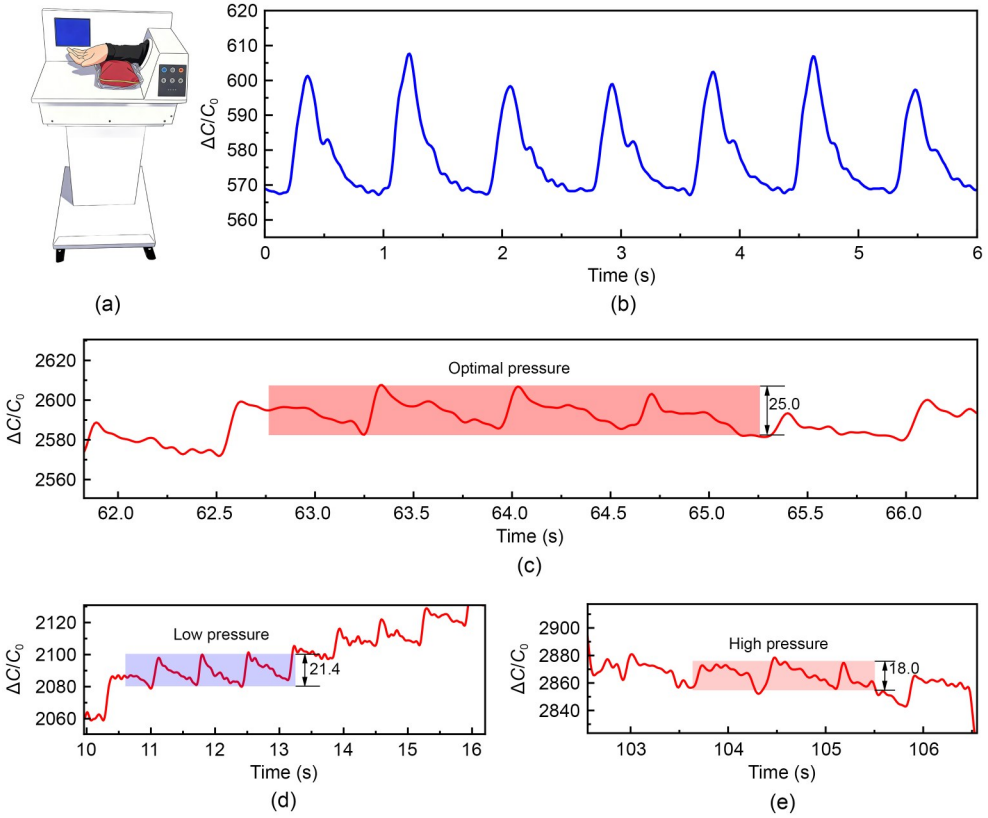


Fig. 4 Pulse detection application of sensor: (a) standard pulse signal instrument; (b) simulated pulse signal; (c–e) actual pulse signals of optimal pressure, low pressure, and high pressure

adhesiveness, and notable stretchability. The ultra-thin and stretchable characteristics enable sensors to maintain high performance after encapsulation, while the ultra-thin characteristic means that encapsulation essentially has no impact on the sensor's performance. Waterproof structural adhesive was incorporated into the edge seams and wire areas of the encapsulated sensors, where water infiltration was a potential concern, to augment their waterproof capabilities.

The detailed implementation of the practical underwater intelligent communication system is shown in Fig. 5a. Deep learning techniques were used to classify the collected Morse code signals. The sensor differentiates between short pressure impulses (denoted

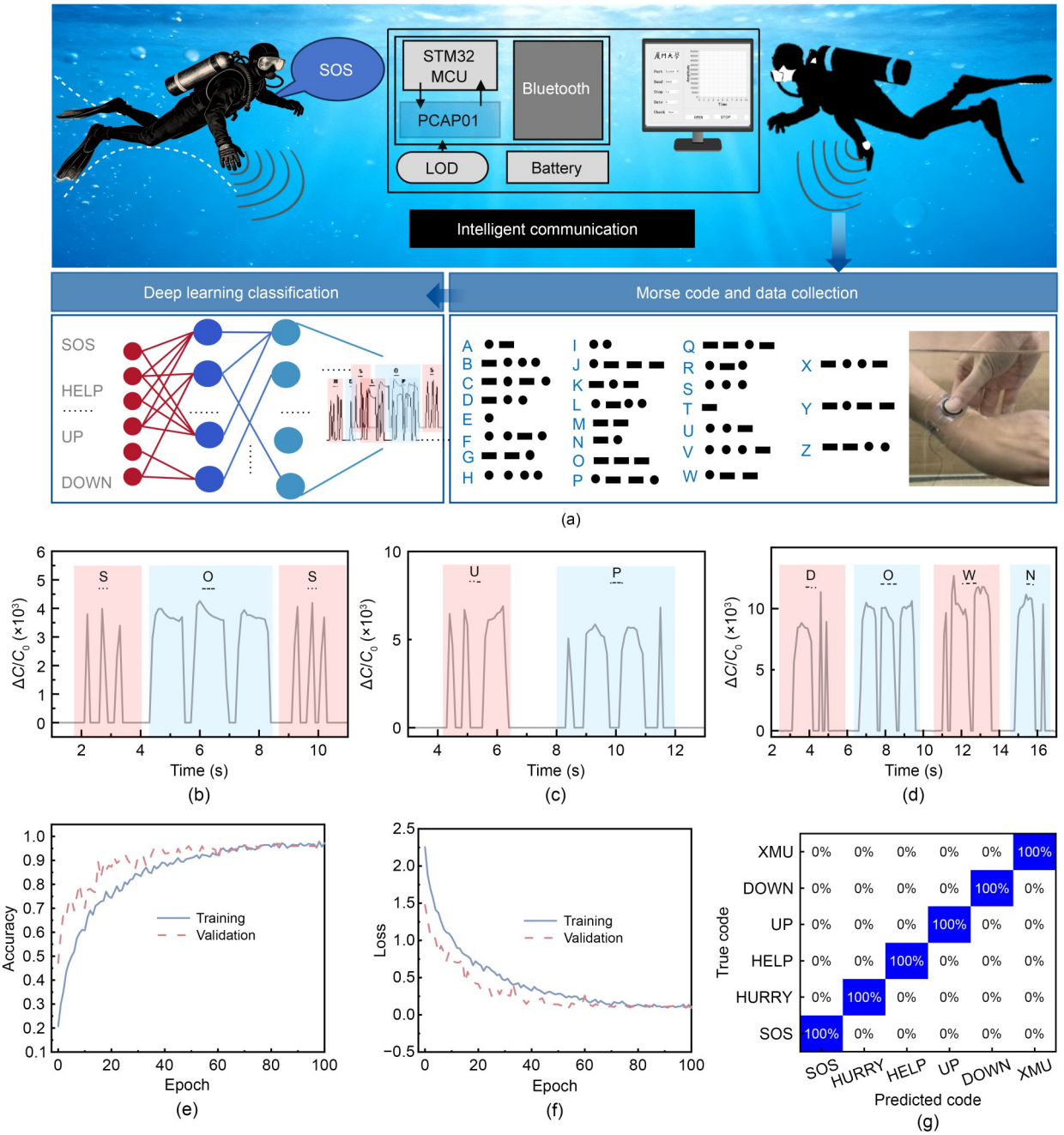


Fig. 5 (a) System design of the underwater intelligent communication; (b–d) sensor output signal diagrams of SOS, UP, and DOWN; (e and f) accuracy and loss during neural network training process; (g) confusion matrix derived from the test set. STM32MCU is the main control chip for backend processing circuits; PCAP01 is the dedicated capacitor to digital conversion signal processor. XMU represents the Xiamen University

by dots) and sustained pressure applications (denoted by dashes), which are combined to generate Morse code. For instance, three rapid taps encode an "S", while three long presses encode an "O", thereby enabling the transmission of the standard "SOS" distress signal (Fig. 5b). Beyond the transmission of basic signals, the conveyance of complex messages is facilitated by the rhythmic tapping of specific letter sequences (Figs. 5c and 5d). A dataset was constructed, incorporating both standard emergent codes (e.g., SOS) and specific command variants labelled "HELP" and "HURRY" (Figs. S6 and S7 of the ESM). The raw sensor output was converted into image formats to serve as inputs for the neural network. A simplified convolutional neural network (CNN) was used for feature extraction and classification. The training metrics showed excellent convergence on both the training and validation sets (Figs. 5e and 5f). The accuracy and loss were highly correlated. In addition, the confusion matrix derived from the test set confirmed superior performance, with zero misclassification (Fig. 5g). Despite the modest size of the current dataset, the outcomes of this study showed the feasibility of the proposed approach. We expect that further performance gains will be realized with the expansion of data collection. To verify the long-term underwater stability of the sensor, a long-term output verification experiment of the sensor in a water tank was conducted. The experimental results (Fig. S8 of the ESM) showed that the sensor displays consistent output for about 3 h underwater, which fulfills the time requirements for single diving and associated activities. This aligns with the initial intended application scenario of the sensor, which pertains to short-term activities such as diving or swimming that may necessitate emergency communication.

In summary, the present study showed the broad potential of the sensor in the domains of underwater safety systems, health monitoring, and intelligent communication interfaces.

4 Conclusions

In summary, this study established a high-performance flexible pressure sensor by iontronic sensing principles and engineered micro-pyramidal architectures. The sensor was developed to achieve ultra-high sensitivity, rapid response and recovery times, and exceptional operational stability by transitioning from traditional parallel-plate capacitive mechanisms to an EDL-based model augmented by interfacial contact area modulation. Moreover, the integration of screen printing with molding provides a scalable fabrication strategy that is well-suited to mass production. The practical utility of the device was systematically validated across diverse domains. In precision healthcare, the sensor showed high-fidelity capture of human pulse waveforms, thereby facilitating the identification of optimal acquisition pressures for non-invasive monitoring. Following hermetic encapsulation, the technology was successfully adapted for aquatic environments. A novel underwater intelligent communication system was demonstrated, which combines tactile Morse code encoding with deep learning-assisted decoding, achieving high accuracy in signal classification. Collectively, this work underscores the immense potential of flexible iontronic sensors in bridging the gap between terrestrial healthcare and aquatic exploration, paving the way for next-generation HMIs and cross-medium intelligent sensing systems.

Acknowledgments

This work is supported by the National Natural Science Foundation of China (Nos. 62274140 and 62405294), the Open Project Fund of Key Lab of Modern Manufacturing Quality Engineering (No. 20250481), China, the Open Research Fund Program of National Key Laboratory of Aerospace Chemical Power (No. NKLACP220241B14), China, the National Key Research and Development Program of China (No. 2023YFB3208600), the Key Program of the National Natural Science Foundation of China (No. 62433017), the Fundamental Research Funds for the Central Universities (No. 20720230030), China, the Xiaomi Young Talents Program/Xiaomi Foundation, the Shenzhen Science and Technology Program (No. JCYJ20230807091401003), China, the Fundamental Research Program of Shanxi Province (No. 202403021222157), China, the Postgraduate Research Innovation Project of Shanxi Province (No. 2024KY583), China, and the International Science and Technology Joint Research Project of Hubei (No. 2024EHA007), China.

Author contributions

Menghui XIANG designed the research. Menghui XIANG and Cong ZHAI processed the corresponding data and wrote the first draft of the manuscript. Congcong HAO and Libo GAO revised and edited the final version. Guirong WU, Jin CHAI, Yunlong ZHAO, Zekai HUANG, Bin YAO, Heying ZHANG, Mengran LIU, Lei NIE, Xiewen WEN, and Chenyang XUE helped to organize and revise the manuscript.

Conflict of interest

Menghui XIANG, Cong ZHAI, Congcong HAO, Guirong WU, Jin CHAI, Yunlong ZHAO, Zekai HUANG, Bin YAO, Heying ZHANG, Mengran LIU, Lei NIE, Xiewen WEN, Chenyang XUE, and Libo GAO declare that they have no conflict of interest.

Declaration on the use of generative AI tools

During the preparation of this work, the authors used DeepSeek to improve language and readability. After using this tool, the authors reviewed and edited the content as needed and take full responsibility for the content of the publication.

Data availability

The data that support the findings of this study are available from the corresponding author upon reasonable request.

References

Cetin O, Cicek MO, Cugunlular M, et al., 2024. MXene-deposited melamine foam-based iontronic pressure sensors for wearable electronics and smart numpads. *Small*, 20(45):2403202. https://doi.org/10.1002/smll.202403202

Chang H, Zhao JZ, Qin R, et al., 2026. Ultra-wideband hybrid triboelectric–piezoelectric acoustic sensors enabled by acoustic metasurface lens for environment perception and medical imaging. *Advanced Functional Materials*, 36(3): e13202. https://doi.org/10.1002/adfm.202513202

Cheng Y, Guo CH, Li S, et al., 2022. Aquatic skin enabled by multi-modality iontronic sensing. *Advanced Functional Materials*, 32(48):2205947. https://doi.org/10.1002/adfm.202205947

Guo JH, Niu Q, Xu JL, et al., 2025. All-in-one iontronic sensing aligner for high-precision 3D orthodontic force monitoring. *Advanced Science*, 12(43):e11984. https://doi.org/10.1002/advs.202511984

Guo XH, Zhao JJ, Hu B, et al., 2024. Flexible pressure sensor with high sensitivity and fast response based on bionic honeycomb-structured polydimethylsiloxane/aluminum oxide composites dielectric via 3-D printing. *IEEE Transactions on Electron Devices*, 71(7):4283-4291. https://doi.org/10.1109/ted.2024.3401653

Hong WQ, Guo XH, Zhang TX, et al., 2023. Flexible capacitive pressure sensor with high sensitivity and wide range based on a cheetah leg structure via 3D printing. *ACS Applied Materials & Interfaces*, 15(39):46347-46356. https://doi.org/10.1021/acsami.3c09841

Jin QX, Wang CY, Wu H, et al., 2024. 3D printing of capacitive pressure sensors with tuned wide detection range and high sensitivity inspired by bio-inspired kapok structures. *Macromolecular Rapid Communications*, 45(9):2300668. https://doi.org/10.1002/marc.202300668

Kurup LA, Arthur JN, Yambem SD, 2022. Highly sensitive capacitive low-pressure graphene porous foam sensors. *ACS Applied Electronic Materials*, 4(8):3962-3972. https://doi.org/10.1021/acsaelm.2c00616

Li KX, Xu TL, Zhou JY, et al., 2025. Flexible capacitive pressure sensor with chemically reduced graphene oxide on a pyramid-structured melamine sponge array by laser engraving. *Journal of Materials Chemistry C*, 13(41):21215-21226. https://doi.org/10.1039/d5tc00563a

Li ZW, Lv T, Wang XW, et al., 2025. High-performance MXene/TPU flexible piezoresistive sensors for enhanced gesture recognition and interactive control applications. *Advanced Materials Technologies*, 10(17):e00613. https://doi.org/10.1002/admt.202500613

Liang JW, Guo HJ, Sun LN, et al., 2025. A nanocrack-based graphene/PDMS-encapsulated medical tape flexible sensor for motion detection of underwater robots. *Advanced Materials Technologies*, 10(20):e00620. https://doi.org/10.1002/admt.202500620

Lin SM, Li XR, Wu YJ, et al., 2025. Load-bearing piezoelectric integrated device with inherent stress monitoring capabilities. *Advanced Functional Materials*, 35(38):2502346. https://doi.org/10.1002/adfm.202502346

Liu HD, Liu C, Luo JN, et al., 2024. Micromesh reinforced strain sensor with high stretchability and stability for full-range and periodic human motions monitoring. *InfoMat*, 6(4):e12511. https://doi.org/10.1002/inf2.12511

Liu LT, Mo LX, Han SB, et al., 2026. Enhancing flexible capacitive sensor performance through the synergy of thermally expandable microspheres and carbon nanotubes via 3D direct ink writing. *Advanced Functional Materials*, 36(9):e14093. https://doi.org/10.1002/adfm.202514093

Lu P, Wang L, Zhu P, et al., 2021. Iontronic pressure sensor with high sensitivity and linear response over a wide pressure range based on soft micropillared electrodes. *Science Bulletin*, 66(11):1091-1100. https://doi.org/10.1016/j.scib.2021.02.019

Lv CY, Tian CC, Jiang JS, et al., 2023. Ultrasensitive linear capacitive pressure sensor with wrinkled microstructures for tactile perception. *Advanced Science*, 10(14):2206807. https://doi.org/10.1002/advs.202206807

Ma R, Zhao YL, Chen HB, et al., 2024. Highly sensitive flexible capacitive pressure sensor with porous hierarchical structure realized by a microwave curing method. *Advanced Engineering Materials*, 26(2):2301412. https://doi.org/10.1002/adem.202301412

Min S, Kim DH, Joe DJ, et al., 2023. Clinical validation of a wearable piezoelectric blood-pressure sensor for continuous health monitoring. *Advanced Materials*, 35(26): 2301627. https://doi.org/10.1002/adma.202301627

Nie BQ, Li RY, Cao J, et al., 2015. Flexible transparent iontronic film for interfacial capacitive pressure sensing. *Advanced Materials*, 27(39):6055-6062. https://doi.org/10.1002/adma.201502556

Nie BQ, Xing SY, Brandt JD, et al., 2012. Droplet-based interfacial capacitive sensing. *Lab on a Chip*, 12(6):1110-1118.

https://doi.org/10.1039/c2lc21168h

Ren JY, Liu YH, Wang ZQ, et al., 2022. An anti-swellable hydrogel strain sensor for underwater motion detection. *Advanced Functional Materials*, 32(13):2107404. https://doi.org/10.1002/adfm.202107404

Sun HL, Li XY, Zhao ZH, et al., 2026. Kirigami cube-inspired triboelectric vector sensor for human–machine interaction. *Advanced Functional Materials*, 36(11):e16876. https://doi.org/10.1002/adfm.202516876

Teng YY, Wang X, Zhang ZD, et al., 2024. Fully printed minimum port flexible interdigital electrode sensor arrays. *Nanoscale*, 16(15):7427-7436. https://doi.org/10.1039/d3nr06664a

Wang X, Wu GR, Zhang XK, et al., 2025. Traditional Chinese medicine (TCM)-inspired fully printed soft pressure sensor array with self-adaptive pressurization for highly reliable individualized long-term pulse diagnostics. *Advanced Materials*, 37(1):2410312. https://doi.org/10.1002/adma.202410312

Wang YH, Xiang MH, Li JH, et al., 2024. Highly sensitive flexible iontronic pressure sensor for marine pressure monitoring. *IEEE Electron Device Letters*, 45(12):2530-2533. https://doi.org/10.1109/led.2024.3474909

Xiang MH, Yu LF, Chai J, et al., 2025. An iontronic pressure sensor with high linearity and ultrawide range over 4 MPa for submarine pressure monitoring. *Chemical Engineering Journal*, 517:164365. https://doi.org/10.1016/j.cej.2025.164365

Xiang QX, Zhao GJ, Tang T, et al., 2025. All-carbon piezoresistive sensor: enhanced sensitivity and wide linear range via multiscale design for wearable applications. *Advanced Functional Materials*, 35(15):2418706. https://doi.org/10.1002/adfm.202418706

Yang CX, Hu JF, Liu LH, et al., 2024. An underwater vest containing an antioxidant MXene hydrogel for sensitive recognition of fish locomotion. *Microsystems & Nanoengineering*, 10(1):41. https://doi.org/10.1038/s41378-024-00675-8

Yang J, Liu Q, Deng Z, et al., 2019. Ionic liquid-activated wearable electronics. *Materials Today Physics*, 8:78-85. https://doi.org/10.1016/j.mtphys.2019.02.002

Yang QQ, Li BQ, Wang MK, et al., 2025. Machine learning-enhanced modular ionic skin for broad-spectrum multimodal discriminability in bidirectional human–robot interaction. *Advanced Materials*, 37(42):e08795. https://doi.org/10.1002/adma.202508795

Yang QQ, Ye ZQ, Wu RK, et al., 2023. A highly sensitive iontronic bimodal sensor with pressure–temperature discriminability for robot skin. *Advanced Materials Technologies*, 8(21):2300561. https://doi.org/10.1002/admt.202300561

Yang ZK, Duan QK, Zang JB, et al., 2023. Boron nitride-enabled printing of a highly sensitive and flexible iontronic pressure sensing system for spatial mapping. *Microsystems & Nanoengineering*, 9(1):68. https://doi.org/10.1038/s41378-023-00543-x

Yang ZK, Zhao YL, Lan YH, et al., 2024. Screen-printable iontronic pressure sensor with thermal expansion microspheres for pulse monitoring. *ACS Applied Materials & Interfaces*, 16(30):39561-39571. https://doi.org/10.1021/acsami.4c05688

Zhang ZY, Yao AF, Raffa P, 2024. Transparent, highly stretchable, self-healing, adhesive, freezing-tolerant, and swelling-resistant multifunctional hydrogels for underwater motion detection and information transmission. *Advanced Functional Materials*, 34(49):2407529. https://doi.org/10.1002/adfm.202407529

Zhao JW, Hu Q, Fu TQ, et al., 2024. Capacitive low-frequency hydrophone based on micronanostructured iontronic hydrogel for underwater monitoring. *ACS Nano*, 18(33):22010-22020. https://doi.org/10.1021/acsnano.4c04094

Zhao YL, Yuan YB, Zhang HY, et al., 2024a. A fully integrated electronic fabric-enabled multimodal flexible sensors for real-time wireless pressure–humidity–temperature monitoring. *International Journal of Extreme Manufacturing*, 6(6):065502. https://doi.org/10.1088/2631-7990/ad6aad

Zhao YL, Sun QX, Mei SX, et al., 2024b. Wearable multichannel-active pressurized pulse sensing platform. *Microsystems & Nanoengineering*, 10(1):77. https://doi.org/10.1038/s41378-024-00703-7

Zhu CJ, Chen GQ, Li SN, et al., 2024. Breathable ultrathin film sensors based on nanomesh reinforced anti-dehydrating organohydrogels for motion monitoring. *Advanced Functional Materials*, 34(52):2411725. https://doi.org/10.1002/adfm.202411725

Electronic supplementary materials

Figs. S1–S8